10.1098/rsta.2002.1158

THE ROYAL SOCIETY

Slow filament dynamics and viscoelasticity in entangled and active actin networks

By Manfred Keller, Rainer Tharmann, Marius A. Dichtl, Andreas R. Bausch and Erich Sackmann

Fakultät für Physik, Technische Universität München, James Franck Straße, 85748 Garching, Germany

Published online 28 February 2003

This paper deals with correlations between the viscoelastic impedance of entangled actin networks and the slow conformational dynamics and diffusive motions of single filaments. The single filament dynamics is visualized and analysed by analysing the Brownian motion of attached colloidal beads, which enables independent measurements of characteristic viscoelastic response times such as the entanglement and reptation times. We further studied the frequency-dependent viscoelastic impedance of active actin–heavy-meromyosin II networks by magnetic-tweezers microrheometry to gain insight into the effect of such highly dynamic and force-generating cross-linkers (exhibiting bond lifetimes of less than 1 s) on the rheological properties. We show that at high frequencies (higher than 1 Hz) the viscoelastic loss modulus is slightly increased relative to the entangled network (associated with an increase in the energy dissipated during mechanical excitations), while at low frequencies the plateau of the impedance spectrum becomes more pronounced as a consequence of the cross-linking of the network and the suppression of the terminal regime. Our data provide evidence that the myosin motor protein may play a role as softener of the actin cortex, enabling the adaptive reduction of the yield stress of cells and thus facilitating cellular deformations.

Keywords: conformational dynamics of actin filaments; semiflexible macromolecules; actin–myosin networks; microrheology

1. Introduction

Numerous chemo-mechanical processes of cells, such as locomotion (crawling) on surfaces, adhesion processes or the engulfment of pathogenic cells by macrophages during immune responses, are mediated by the actin-based cytoskeleton. In quiescent cells this subfraction of the cytoskeleton consists of a rather homogeneous shell several hundred nanometres thick composed of partly cross-linked actin filaments: the actin cortex. In activated cells, the actin skeleton undergoes drastic, often localized, structural changes and it can become highly heterogeneous. These structural changes have to occur often in the time-scale of seconds or faster. Prominent examples are (i) the activation of blood platelets during the initial step of wound healing (Lodish *et al.* 1999); (ii) contraction of endothelial cells within the confluent cell

One contribution of 14 to a Discussion Meeting 'Slow dynamics in soft matter'.

monolayer lining the inner wall of blood vessels to enable migration of lymphocytes from the blood into the tissue invaded by pathogens (Garcia & Schaphorst 1995); and (iii) the stabilization of cell adhesion by formation of focal contacts (Smilenov *et al.* 1999). In all these cases, the structural reorganization consists of the formation of actin bundles within the actin cortex which can serve as stress fibres to stabilize the cell shape or as contractile cables (mini muscles) to generate gaps within the endothelial cell layers by centripetal contraction of individual cells (Hillebrandt *et al.* 2001). Another prominent example is the advancement of protrusions by unidirectional growth of strongly cross-linked actin gel which drives the formation of pseudopodia and filopodia or provides the driving force for the motion of *Lysteria* bacteria in cells (Prost 2002).

These rapid structural changes are mediated by several families of actin-manipulating proteins (Lodish *et al.* 1999). These include (i) monomer-sequestering proteins to control the fraction of actin polymerized (and therefore the mesh size of the network); (ii) capping proteins which bind to the fast-growing end of filaments thus limiting the filament contour length L; (iii) membrane-coupling proteins that mediate the binding between actin filaments and intracellular domains of cell adhesion molecules (such as integrin); and (iv) actin cross-linking molecules. The family of cross-linkers consists of several structurally different subgroups including rod-like linkers (such as α-actinin), exhibiting actin binding sites at both ends, and fork-like connectors (such as filamin), exhibiting binding sites at the ends of the prong. The latter subgroup also includes the muscle protein myosin II, which can act in cells as a force generator and cross-linker. An important feature of the cross-linkers is the kinetics of the actin-linker binding equilibrium. Thus, filamin (from muscle) and α-actinin are weak linkers exhibiting binding energies of a few $k_{\mathrm{B}}T$ at room temperature and off-rates of *ca.* 0.5 s. Myosin is also a weak linker in the presence of adenosine triphosphate (ATP) but exhibits strong binding to actin in the absence of ATP (rigour-state situation).

The dynamic control of the molecular architecture of the actin cortex (such as actin bundling in endothelial cells, triggered by inflammation signal molecules such as thrombin (Bausch *et al.* 2001)) occurs through activation or inhibition of the actin-manipulating proteins by second messengers such as Ca^{2+} or through phosphorylation and dephosphorylation reactions (cf. Sackmann *et al.* 2002). Ca^{2+}, for instance, can activate the severing protein gelsolin, thus promoting gel–sol transitions. The phosphorylation is mediated by proteins called kinases, which are activated by guanosine 5′-triphosphate (GTP)-cleaving proteins called G-proteins. Since an external signal (e.g. the binding of a hormone to a receptor) can liberate bursts of Ca^{2+} ions from intracellular Ca^{2+} stores or a G-protein can activate many kinases, the signals are amplified dramatically (Hall 1998).

Numerous cell-biological studies of normal cells and mutants lacking one or several actin regulation proteins, including myosins, yielded insight into the biochemical basis of the actin-cortex reorganizations and their role for chemo-mechanical shape changes of cells (Schindl *et al.* 1995; Condeelis & Vahey 1982; De Lozanne & Spudich 1987). Experiments with micromechanical tools provided some information on correlations between the architecture of the actin cortex and the viscoelastic moduli of the cell envelope (Bausch *et al.* 2001; Schindl *et al.* 1995). They also showed that mechanical forces can induce reorganizations of the actin cytoskeleton such as force-induced growth of protrusions (Zheng *et al.* 1991).

Another hopeful approach towards an understanding of correlations between the architecture of the actin cytoskeleton and the mechanical properties of cells is based on the design of more and more realistic models of the actin cortex (cf. Limozin & Sackmann 2002) and the systematic study of the viscoelastic properties and molecular dynamics of such mechanical *in vitro* models of cells. Owing to the distinct physical properties of single actin filaments or networks of this semiflexible macromolecule, such studies are also of great interest from the point of view of polymer research.

The present work concentrates on one aspect of the rich physics of the actin-based cytoskeleton: the correlation between viscoelastic properties of (homogeneous) actin networks and the slow molecular dynamics of single filaments. We do not consider the more realistic situation of heterogeneous networks. The reader is referred to Tempel *et al.* (1996) and a review by Sackmann *et al.* (2002).

2. Basic properties of actin filaments and networks

Polymerized actin is a prototype of a semiflexible macromolecule composed of double-stranded filaments several 10 μm in length (in an appropriate buffer containing Ca^{2+} and Mg^{2+}, called F-buffer). It is a living polymer, which coexists in a stationary equilibrium with globular monomers ('G-actin', 42.000 Da). The filaments (called 'F-actin') exhibit a fast-growing end (ratio of monomer on-rate to off-rate $k_{\mathrm{on}}/k_{\mathrm{off}} \sim 10$) and a slowly growing end with $k_{\mathrm{on}}/k_{\mathrm{off}} \sim 0.1$. In polymerizing solution (F-buffer), F-actin forms random (orthogonal) networks with well-defined mesh size ξ (the average shortest distance between filaments), which is a consequence of the pronounced thermally excited bending fluctuations.

The static structure and elasticity is characterized by three length-scales. The filament contour length (L), the mesh size of the network (ξ) and the persistence length of the filaments (L_{P}). L_{P} is defined as the decay length of the exponentially decaying correlation between the orientations of the tangents $\boldsymbol{t}$ to the filament at two positions s and s' of the filament: $\langle \boldsymbol{t}(s')\boldsymbol{t}(s)\rangle = \exp(-|s-s'|/L_{\mathrm{P}})$. $|s-s'|$ is the distance between the two positions along the contour of the filament. Under physiological salt conditions (100 mM KCl), the persistence length is *ca.* 17 μm but L_{P} can be smaller at low ionic strength ($L_{\mathrm{P}} = 10$ μm at 10 mM KCl; cf. Isambert *et al.* 1995). L_{P} can also change by binding of actin-manipulation proteins such as tropomyosin, a 40 nm long rod-like protein binding into the groove formed between the two twisted protofilaments (Götter *et al.* 1996). The persistence length is related to the filament-binding modulus B according to

$$B = k_{\mathrm{B}} T L_{\mathrm{P}}. \tag{2.1}$$

The dynamic properties and viscoelasticity of actin networks are determined by the thermally excited bending fluctuations (the dynamic roughness) of the actin filaments, which are best described in terms of Fourier modes

$$U(s,t) = \sum_q U_q(t)\exp(\mathrm{i}qs), \quad q = n\pi/L, \quad n \in \boldsymbol{N}.$$

We obtain the amplitudes $U_q(t)$ from the equipartition theorem ($U_q^2 = k_{\mathrm{B}}T/Bq^4L$), and the dynamic filament roughness is then best characterized by the mean-square amplitude $\langle u^2\rangle$ (called roughness) depending on the contour length as

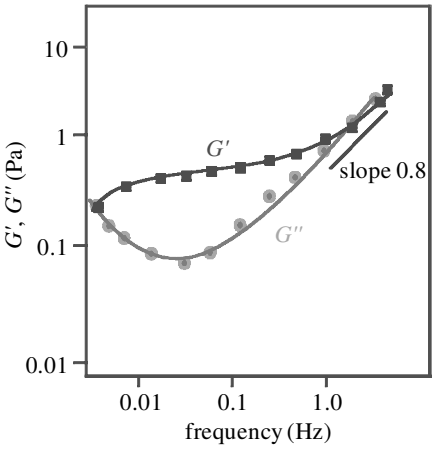

Figure 1. Viscoelastic impedance spectra $G'(f), G''(f)$ of purely entangled actin network exhibiting three frequency regimes: (i) the tension-dominated regime at $f > \tau_e^{-1}$; (ii) the plateau regime at medium frequencies; and (iii) the terminal regime at $f < \tau_d^{-1}$. Note that only the high-frequency onset of the terminal regime is seen. Measurement was made by magnetic tweezers microrheometry with 4.5 μm superparamagnetic beads (cf. Keller *et al.* (2001)). Actin concentration is 2 mg ml^{-1}.

$\langle u^2 \rangle = k_B T L^3/B$. (For $L \sim 1$ μm (or 0.1 μm), $\sqrt{\langle u^2 \rangle} \approx 0.3$ μm (or 0.01 μm), which is *ca.* 300 (or 2) times the filament thickness.) An important consequence of the dynamic roughness of the filament is that it gives rise to an entropic tension τ (MacKintosh *et al.* 1995), which depends, however, strongly on the bending modulus B according to

$$\tau \approx \left(\frac{B^2}{k_B T L^4}\right)\delta L,$$

where δL is the length change. However, due to the semiflexible nature of the filaments, τ depends on the orientation of an applied force with respect to the filament axis (in striking contrast to flexible filaments) (Frey 2002).

Due to their semiflexible character, the filaments can (easily) buckle under forces parallel to the filament axis. According to the Euler theory, the critical force (at $L \ll L_P$) is $f_c \approx \pi^2 B/L^2$. Note that $f_c \approx 0.3$ pN for $L \approx 1$ μm or $f_c \approx 30$ pN for $L \approx 0.1$ μm (the typical mesh size of the actin cortex). The Euler instability may thus play an important role in the elasticity of the actin cortex.

3. Viscoelasticity of homogeneous actin networks

The most important property of the actin cortex for its role as the chemo-mechanical machine of cells is its viscoelasticity in the slow (hydrodynamic) time regime (10^{-2}–10^4 s). The frequency-dependent viscoelastic impedance $G^*(f) = G'(f) + iG''(f)$ (G' is the storage modulus and G'' the loss modulus) has been extensively studied by torsional macrorheometry (Hinner *et al.* 1998) and magnetic tweezers (Keller *et al.* 2001) or colloidal probe (Crocker *et al.* 2000) microrheometry. Typical frequency spectra of $G'(f)$ and $G''(f)$ taken by magnetic bead microrheometry are shown in figure 1. Three frequency regimes can be distinguished which can be attributed to well-defined molecular processes: (i) a fast regime $f > \tau_e^{-1}$ (τ_e is the entanglement

time defined below), which is determined by the entropic tension of the filaments; (ii) a plateau regime at $\tau_{\rm d}^{-1} < f < \tau_{\rm e}^{-1}$ ($\tau_{\rm d}$ is the terminal relaxation time) associated with the affine deformation of the network; and (iii) the terminal regime at $f < \tau_{\rm d}^{-1}$, where the network starts to flow by self-diffusion of the filaments. A rather rigourous theory of the viscoelastic modulus $G^*(f)$ based on a modified Doi–Edwards tube model was derived by Morse (1998*a*, *b*) and astonishingly good agreement with experimental data was demonstrated (Morse 1998*c*).

The cross-over times $\tau_{\rm e}$ and $\tau_{\rm d}$ have well-defined meanings. $\tau_{\rm d}$ is the disengagement time, which is equal to the time a filament requires to diffuse over a distance equal to its contour length and is therefore also called the reptation time $\tau_{\rm rept}$. It was related to the self-diffusion coefficient $D_{\rm rept}$ of the filaments by Morse (1998*b*), $\tau_{\rm rept} = L^2/\pi^2 D_{\rm rept} \propto L^3$. $\tau_{\rm e}$ is the relaxation time (also-called 'entanglement time') of the longest wavelength bending mode of a single filament that is not truncated by the constraints imposed by the other chains of the networks (or the wall of the tube). In the framework of the Edwards–de Gennes tube model (de Gennes 1979), this constraint is accounted for by the width of the primitive tube, which is of the order of the mesh size. The maximum wavelength $\Lambda_{\rm e}$, called the entanglement length ($L_{\rm e} \approx \Lambda$), is obtained from the roughness $\langle u^2 \rangle$ defined above. The entanglement time is given by (Isambert & Maggs 1996)

$$\tau_{\rm e} \approx \frac{\zeta_\perp L_{\rm e}^4}{B} \approx \frac{\zeta_\perp L_{\rm p}^{1/3} d^{8/3}}{k_B T}, \tag{3.1}$$

where $\zeta_\perp$ is the friction coefficient of the filament within the tube and d is the tube diameter.

An important parameter is the plateau modulus (which is a measure for the shear modulus of the network). For purely entangled networks it is determined by the mesh size ξ, the entanglement length $L_{\rm e}$ and the bending modulus B:

$$G^0_{\rm entangle} = \frac{\frac{9}{5} k_{\rm B} T}{\xi^2 L_{\rm e}} \approx \frac{k_{\rm B} T}{L_{\rm P}^{1/5} \xi^{14/5}}. \tag{3.2}$$

This power law has been verified experimentally (Hinner *et al.* 1998). In the approximation of stiff chains the mesh size is related to the concentration of actin monomers $c_{\rm A}$ by $\xi \propto 1/\sqrt{c_{\rm A}}$. This equation has also been verified experimentally (Schmidt *et al.* 1989). Note that $\xi \approx 0.5$ μm for $c_{\rm A} = 0.4$ mg ml^{-1} (9.5 μM). For fully cross-linked networks the entanglement length $L_{\rm e}$ is approximately equal to the mesh size ($L_{\rm e} \approx \xi$) and the shear modulus depends much more strongly on the chain stiffness (Gittes & MacKintosh 1998),

$$G^0_{\rm link} = \frac{k_{\rm B} T L_{\rm P}^2}{\xi^5}. \tag{3.3}$$

The ratio

$$\frac{G^0_{\rm link}}{G^0_{\rm entangle}} \sim \left(\frac{L_{\rm P}}{\xi}\right)^{11/5} \tag{3.4}$$

is thus always larger than one. Note that for partly cross-linked networks $G_{\rm link} \approx G_{\rm entangle}$, as verified for actin–α-actinin networks. If the linker density is approximately equal to or higher than the density of naturally occurring cross-links, the network becomes heterogeneous (Tempel *et al.* 1996). For dynamic (and thus reversible)

cross-linkers such as α-actinin, the network undergoes a reversible percolation-like transition into a hetero-gel and the shear elastic modulus diverges.

4. Experimental verification of power laws

(*a*) *Tube width measurements*

The power laws summarized above have been tested by comparison of impedance spectra measured by torsional rheometry and calculated by application of the Doi–Edwards tube model (Doi & Edwards 1986) to semiflexible macromolecules by Morse (2001). Good agreement was obtained for the plateau modulus and the tension-dominated high-frequency regime, while the frictional coupling $\zeta_\perp$ obtained by this comparison is an order of magnitude smaller than the value measured by enforced reptation studies of single filaments by the technique of magnetic tweezers (Dichtl & Sackmann 2002). The power law (equation (3.2)) relating the plateau modulus to the mesh size or the actin concentration c_A ($\xi \sim c_\mathrm{A}^{-1/2}$) has also been verified (Hinner *et al.* 1998).

Another strategy to evaluate the scaling laws (allowing us to relate the macroscopic viscoelastic parameters to filament motional processes) is based on the Brownian motion analysis of test filaments labelled by fluorescent chromophores or nano gold beads (Dichtl & Sackmann 1999, 2002).

Two examples are presented in figures 2 and 3. Figure 2 shows a measurement of the local variation of the tube width d by analysis of the transverse fluctuations of a fluorescent test filament. By analysing the fluorescence intensity distribution along sections perpendicular to the local tube axis (which can be represented as Gaussian distributions), the tube width is determined by the variance of the distribution along the tube direction. In the example shown, the tube width varies only slightly along the filament axis but much larger variations occur frequently (Dichtl & Sackmann 2002). In a previous study, it was shown that the tube width can also be determined locally by measuring distributions $P(\Delta y^2(t))$ of the mean-square displacement (MSD) of colloidal beads coupled to the filament perpendicular to the tube axis. The interaction potential characterizing the coupling of the test filament with the environment is then obtained by the Boltzmann law $V_\mathrm{tube} = -k_\mathrm{B}T \ln\{P(\Delta y^2(t))\}$ (Dichtl & Sackmann 1999). Taken together, these studies showed that the tube width can vary locally by a factor of two (for physiological salt concentrations of *ca.* 100 mM KCl). Smaller variations have been found at lower ion concentrations (less than 10 mM KCl) and phalloidin-stabilized filaments.

The analysis of figure 2*a* showed that at short times ($t < \tau_\mathrm{e}$) the motion of the local segment of the filament (as probed by the colloidal bead) is astonishingly isotropic. At $t > \tau_\mathrm{e}$, the MSD in the normal direction saturates, while in the tangential direction it increases linearly with time at $t > \tau_\mathrm{e}$. Since the gold beads can be observed over a very long time (in contrast to fluorescent filaments), reliable values of the reptation diffusion constant D_rept can be measured. The reptation times $\tau_\mathrm{R} = L^2/2D_\mathrm{rept}$ obtained in this way agree well with the terminal relaxation time τ_d (Dichtl & Sackmann 2002).

The coefficient of tangential friction ζ exerted on the filament by the wall of the tube can be related to the effective viscosity of the fluid in the tube. In the rigid-rod

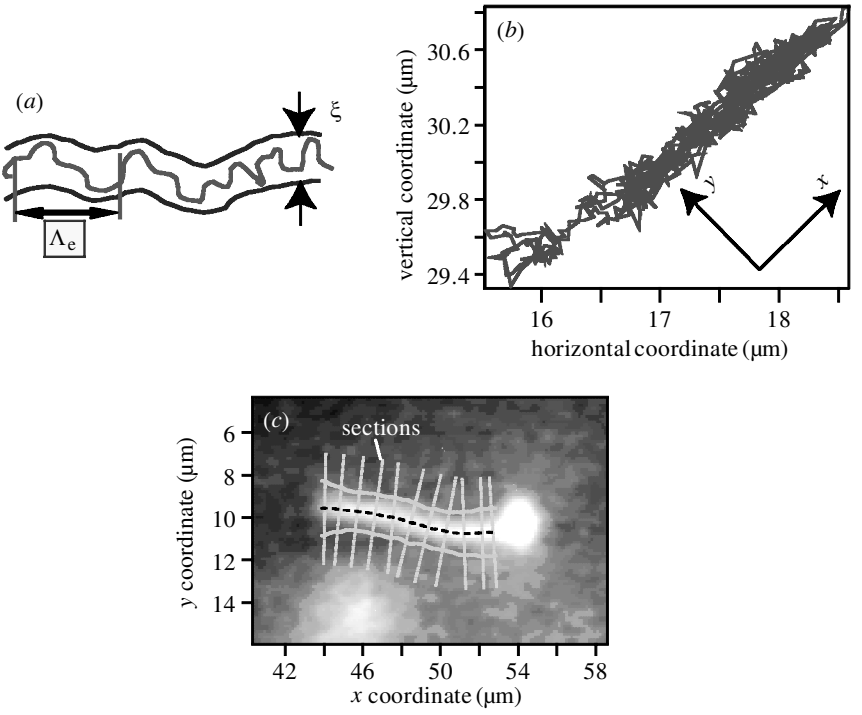

Figure 2. (*a*) Definition of reptation tube and entanglement length. (*b*) Random walk of a colloidal gold bead (17 nm in diameter) coupled to a test filament observed for *ca.* 100 s, which demonstrates the anisotropic motion of the local segment of the filament in the reptation tube. From these data, the MSDs parallel and perpendicular to the tube axis are obtained as described in Dichtl & Sackmann (2002). Note that the motion of the colloidal bead can be observed by confocal ultra microscopy with *ca.* 5 nm spatial resolution and 4 ms time resolution. (*c*) Local measurement of tube width from the MSD of a single filament as described in the text.

approximation

$$\zeta = \frac{k_{\mathrm{B}}T}{D_{\mathrm{rept}}L} = \frac{2\pi\eta_{\mathrm{s}}}{\ln\{\Lambda/a\}},$$

where η_{s} is the effective viscosity of the solvent in the tube, Λ is the so-called hydrodynamic screening length and is of the order of the mesh size and a is the filament diameter. A strange yet not understood result of the analysis of the self diffusion on the basis of the above model is that the solvent viscosity is at least an order of magnitude larger than the value for water ($\eta_{\mathrm{s}} = 10^{-3}$ J s m^{-3}) (Dichtl & Sackmann 2002).

(*b*) *Measurement of entanglement times* τ_{e} *from segmental mean-square displacements*

The analysis of the Brownian motion of colloidal beads coupled to test filaments also provides an independent tool to measure the entanglement time τ_{e} besides the macroscopic measurement of τ_{e} by viscoelastic impedance spectroscopy. τ_{e} is obtained from the saturation time of the MSD-versus-time plots. Two examples are shown in figure 3*a*. This allows us to measure τ_{e} as a function of the tube diameter to test

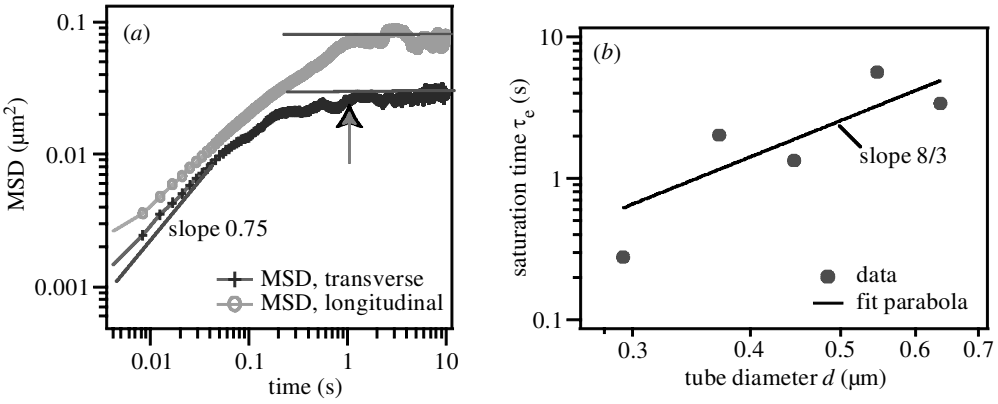

Figure 3. (*a*) Short-time MSD parallel ($\Delta x^2(t) = \langle |x(t) - x(0)|^2 \rangle$) and perpendicular ($\Delta y^2(t)$) to the tube axis by analysis of Brownian motion of nano gold beads (17 nm in diameter) or 35 nm fluorescent latex beads coupled to the filament by biotin–avidin–biotin linkage. The curves saturate at the entanglement relaxation time τ_e. The initial slope is $\Delta x^2(t) \sim \Delta y^2(t) \sim t^{3/4}$. Note that the longitudinal MSD ($\Delta x^2(t)$) extends linearly with time at long times $t \gg \tau_e$ (from Dichtl & Sackmann (1999)). (*b*) Plot of entanglement time τ_e obtained from the saturation time of the MSD of colloidal beads perpendicular to the tube axis. The solid line corresponds to the scaling law $\tau_e \propto d^{8/3}$ as predicted by Isambert & Maggs (1996).

the scaling law (equation (3.1)) for τ_e, since the tube width can be simultaneously measured by the technique of figure 2. As shown in figure 3*b*, the law $\tau_e \propto d^{8/3}$ is reasonably well fulfilled.

5. Active actin–heavy-meromyosin networks

Myosin is an ubiquitous motor protein in most eucaryotic cells. In the quiescent state (for instance, of amoeba-like cells of the slime mould *Dictyostelium discoideum*), the motor proteins are not bundled (as in the muscle) and are randomly distributed throughout the cytoplasm. Myosin accumulates, however, in the cortex region of the trailing end of cells crawling on surfaces or in retracting protrusions enforced by local external forces (Merkel *et al.* 2000). Interestingly, it has been shown (for the case of *Dictyostelia* cells) that the state of aggregation of myosin is controlled by phosphorylation of amino acids in the 130 nm long tail of the myosin molecule. In the dephosphorylated state, the tails are stretched and can form bundles, while after phosphorylation the tails are bent in the middle, thus preventing aggregation (Pasternak *et al.* 1989). These findings suggest that myosin can play a dual role as a motor protein in contractile structures and as an active cross-linker that controls the softness (yield stress) of the cell envelope. Evidence for such a role has been provided by micro-mechanical studies of the local yield stress required to disrupt the plasma membrane from the actin cortex, which showed that this yield force is by a factor of five smaller for wild-type *Dictyostelia* cells than for mutants lacking myosin II. The higher stability of the mutant is attributed to the replacement of myosin by other cross-linkers exhibiting higher binding strengths.

To gain insight into the role of myosin motors as active cross-linkers, we studied the impedance spectra of actin networks cross-linked by myosin II and its heavy meromyosin (HMM) fragments lacking a part of the long tail. Both molecules exhibit

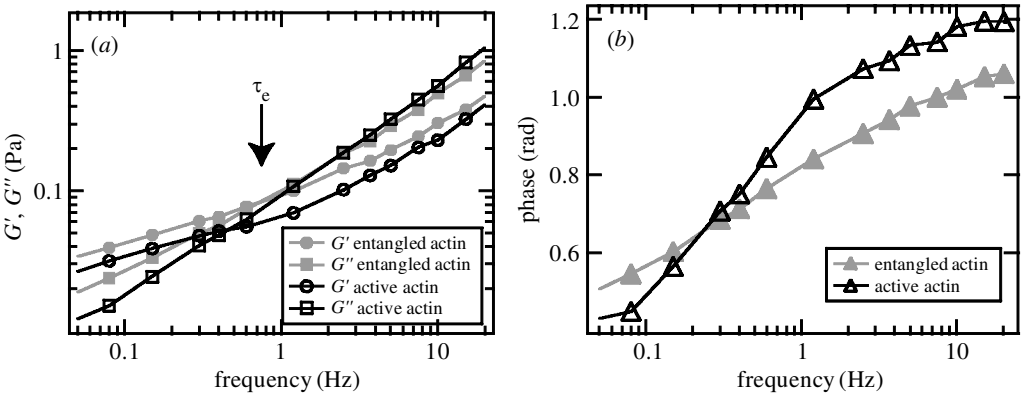

Figure 4. (*a*) Comparison of frequency spectra of the viscoelastic moduli ($G'(f)$ and $G''(f)$) of entangled and HMM-cross-linked (actin-to-myosin molar ratio of 54) network. Small but remarkable differences are found, notably a relative increase in the loss modulus in the tension-dominated regime and the appearance of a more pronounced plateau of $G'(f)$ at $f < 0.1$ Hz. (*b*) Comparison of frequency dependence of the loss angle for the two networks. The tangent of loss angle ($\tan\varphi = G''(f)/G'(f)$) is a measure of the ratio of the energy dissipated to the energy stored during one cycle.

fork-like structures with actin binding sites at both heads. We performed measurements with both magnetic-bead microrheometry and torsional macrorheometry.

Figure 4*a* shows the result for the HMM fragment obtained by microrheometry. The frequency spectra of the viscoelastic parameters for purely entangled actin and actin–HMM networks are compared. Due to the substantial fluctuations in the local mesh size mentioned above, the absolute values of the moduli cannot be distinguished. However, the shape of the spectra exhibit distinct differences. First, the viscoelastic loss modulus $G''(f)$ is slightly shifted to higher values in the tension-dominated regime. Secondly, although it appears that the network is softened in the low-frequency regime, it is seen that the plateau becomes more pronounced (or the network becomes more elastic) in the presence of HMM. A more reliable and more direct physical insight into the effect of the motor protein is gained by considering the loss angle $\varphi(f) = \arctan(G''(f)/G'(f))$, shown in figure 4*b*. It is shifted to higher values at $f > f_e$, but is decreased in the low-frequency regime (in the plateau). $\tan\varphi$ is a measure for the ratio of the energy dissipated to the energy stored during one cycle of the oscillation. The higher-energy dissipation in the tension-dominated regime can be attributed to the fact that transient actin–HMM bonds between single filaments and the wall of the tube have to be broken to stretch the filament. The decrease in φ at low frequency indicates a more elastic behaviour of the actin network cross-linked by HMM, as expected from the finding of a more pronounced plateau, suggesting that the terminal fluid-like behaviour of the dynamically cross-linked networks is suppressed.

In summary, HMM induces a small but remarkable modification of the entangled actin network, notably an increase in the energy dissipation in the tension-dominated regime and a more elastic behaviour at low frequencies.

Similar behaviour was found for actin–myosin II networks in the presence of buffer which prevents formation of myosin minifilaments. The actin–myosin network is homogeneous in the presence of ATP and for myosin densities smaller than the

density of naturally occurring points of entanglement. Again microrheological studies suggest some hardening in the tension-dominated frequency regime and the formation of a plateau in the low-frequency regime $f \gtrsim \tau_{\mathrm{d}}^{-1}$. For the homogeneous networks we do not find evidence for an increase in the reptation time as reported by Humphrey *et al.* (2002) for actin networks in the presence of myosin minifilaments. Note, however, that in both experiments different buffers were used, resulting in different organizations of myosin. In summary, both motor proteins myosin II and its HMM fragment induce small but reproducible and characteristic changes of slope of the impedance spectra: a relative increase in the loss modulus in the tension-dominated regime and the appearance of a more pronounced plateau of $G'(f)$ close to the terminal regime. This holds for homogeneous networks when the density of linkers is less than or equal to the density of naturally occurring cross-links. The situation changes at much higher cross-linker density (above the percolation threshold), where the network becomes heterogeneous in analogy to the behaviour of actin–α-actinin networks (M. Keller *et al.* 2002, unpublished research).

The relatively small increase in the plateau modulus can be explained in terms of the scaling law of equation (3.2) ($G_0' \sim k_{\mathrm{B}}T/\xi^2 L_{\mathrm{e}}$). This equation holds for entangled and weakly cross-linked networks if the deformation is small so that the excess length due to the dynamic roughness of the chain is not pulled out (MacKintosh *et al.* 1995). The entanglement length $L_{\mathrm{e}} \sim \xi^{2/3} L_{\mathrm{P}}^{1/3}$ is reduced due to the cross-linking of naturally occurring points of entanglement since L_{e} must be equal to or less than the average distance d_{CC} between rigid cross-links. For an actin-to-myosin molar ratio $r_{\mathrm{AC}} = 160$, d_{CC} is *ca.* 0.5 μm. However, in the presence of ATP, only a fraction γ of the cross-links is active. γ is similar to the duty ratio, which is the fraction of time the motor protein is bound to actin during the whole chemo-mechanical cycle. At excess ATP, $\gamma \approx 0.05$ (Duke & Leibler 1996). Thus the distance between bound cross-linkers is $d_{\mathrm{CC}}/\sqrt{\gamma}$ on average. For $r_{\mathrm{AC}} = 160$, $d_{\mathrm{CC}}/\sqrt{\gamma} \sim 2$ μm. This is approximately equal to the value of the entangled network $L_{\mathrm{e}} = \xi^{2/3} L_{\mathrm{P}}^{1/3} \sim 1.5$ μm. This numerical consideration shows that the effect of the cross-linkers is indeed expected to be small for small deformations or stresses smaller than the yield stress.

6. Conclusions

Networks of the semiflexible actin filament (F-actin) are not only of interest owing to their important role in numerous chemo-mechanical cellular processes but also from the point of view of polymer physics. Due to the semiflexibility of actin, the networks exhibit distinct and non-universal viscoelastic properties which depend sensitively on the filament bending modulus and on the mesh-size-dependent entanglement length. The analysis of the single-filament conformational dynamics and Brownian motion of local segments parallel and perpendicular to the tube axis provides a microscopic tool (besides rheometry) to measure characteristic viscoelastic response times such as the entanglement and terminal relaxation time and to relate these to distinct molecular relaxation processes.

Cross-linking of the entangled actin network by the dynamic and active cross-linker myosin II (or its HMM fragment) at densities smaller than or equal to the density of naturally occurring cross-links induces a slight increase in the loss modulus (and thus in the dissipated energy) in the frequency regime dominated by the filament tension.

At low frequencies the network exhibits elastic behaviour and the terminal fluid-like behaviour is suppressed due to cross-linking. The motor proteins thus behave very similarly to α-actinin (Tempel *et al.* 1996), which is also a weak cross-linker, exhibiting an off-rate of $0.4\ \mathrm{s}^{-1}$ of the actin–α-actinin bond. Due to this weak binding, the network behaves as a viscoplastic body exhibiting flow-like behaviour under constant external creep forces.

By establishing scaling laws relating the viscoelastic moduli to structural parameters of the network (ζ, L_e, B), the results obtained for microscale networks can be applied to draw quantitative conclusions concerning the viscoelastic impedance of the actin cortex which exhibits mesh sizes in the 100 nm regime. In fact, it has been established that the scaling law of equation (3.2) holds for mesh sizes between 1 μm and 0.2 μm (Hinner *et al.* 1998). Another important parameter to be considered in this context is the finite size of the intracellular actin network. To study such finite size effects actin networks have been reconstituted into giant vesicles (Limozin & Sackmann 2002).

We acknowledge technical help by M. Rusp and fruitful discussions with E. Frey, D. Morse and F. MacKintosh. Financial support by the Deutsche Forschungsgemeinschaft and the Fonds der Chemischen Industrie. Partial support by the NSF (USA, grant no. Phy99-07949) and the hospitality of the Institute for Theoretical Physics at the University of California Santa Barbara is also gratefully recognized by E.S. and A.B.

References

Bausch, A. R., Hellerer, U., Essler, M., Äpfelbacher, M. & Sackmann, E. 2001 Rapid stiffening of integrin receptor–actin linkages in endothelial cells stimulated with thrombin: a magnetic bead microrheology study. *Biophys. J.* **80**, 2649–2657.

Condeelis, J. & Vahey, M. 1982 A calcium- and pH-regulated protein from dictyostelium discoideum that cross-links actin filaments. *J. Cell Biol.* **94**, 466–471.

Crocker, J. C., Valentine, M. T., Weeks, E. R., Gisler, T., Kaplan, P. D., Yodh, A. G. & Weitz, D. A. 2000 Two-point microrheology of inhomogeneous soft materials. *Phys. Rev. Lett.* **85**, 888–891.

de Gennes, P.-G. 1979 *Scaling concepts in polymer physics*. Ithaca, NY: Cornell University Press.

De Lozanne, A. & Spudich, J. A. 1987 Disruption of the dictyostelium myosin heavy chain gene by homologous recombination. *Science* **236**, 1086–1091.

Dichtl, M. A. & Sackmann, E. 1999 Colloidal probe study of short time local and long time reptational motion of semiflexible macromolecules in entangled networks. *New J. Phys.* **1**, 18.1–18.11. (Available from http://www.njp.org.)

Dichtl, M. A. & Sackmann, E. 2002 Microrheometry of semiflexible actin networks through enforced single-filament reptation: frictional coupling and heterogeneities in entangled networks. *Proc. Natl Acad. Sci. USA* **99**, 6533–6538.

Doi, M. & Edwards, S. F. 1986 *The theory of polymer dynamics*. Oxford: Clarendon Press.

Duke, T. & Leibler, S. 1996 Motor protein mechanics: a stochastic model with minimal mechanochemical coupling. *Biophys. J.* **71**, 1235–1247.

Frey, E. 2002 Physics in cell biology: on the physics of biopolymers and molecular motors. *ChemPhysChem* **3**, 270–275.

Garcia, J. G. & Schaphorst, K. L. 1995 Regulation of endothelial cell gap formation and paracellular permeability. *J Investig. Med.* **43**, 117–126.

Gittes, F. & MacKintosh, F. C. 1998 Dynamic shear modulus of a semiflexible polymer network. *Phys. Rev.* E **58**, R1241–R1244.

Götter, R., Kroy, K., Frey, E., Bärmann, M. & Sackmann, E. 1996 Dynamic light scattering from semidilute actin solutions: a study of hydrodynamic screening, filament bending stiffness and the effect of tropomyosin/troponin-binding. *Macromolecules* **29**, 30–36.

Hall, A. 1998 Rho GTPases and the actin cytoskeleton. *Science* **279**, 509–514.

Hillebrandt, H., Abdelghani, A., Abdelghani-Jacquin, C., Aepfelbacher, M. & Sackmann, E. 2001 Electrical and optical characterization of thrombin-induced permeability of cultured endothelial cell monolayers on semiconductor electrode arrays. *Appl. Phys.* A **73**, 539–546.

Hinner, B., Tempel, M., Sackmann, E., Kroy, K. & Frey, E. 1998 Entanglement, elasticity, and viscous relaxation of actin solutions. *Phys. Rev. Lett.* **81**, 2614–2617.

Humphrey, D., Duggan, C., Saha, D., Smith, D. & Käs, J. 2002 Active fluidization of polymer networks through molecular motors. *Nature* **416**, 413–416.

Isambert, H. & Maggs, A. C. 1996 Dynamics and rheology of actin solutions. *Macromolecules* **29**, 1036–1040.

Isambert, H., Venier, P., Maggs, A. C., Fattoum, A., Kassab, R., Pantaloni, D. & Carlier, M. F. 1995 Flexibility of actin filaments derived from thermal fluctuations. Effect of bound nucleotide, phalloidin, and muscle regulatory proteins. *J. Biol. Chem.* **270**, 11 437–11 444.

Keller, M., Schilling, J. & Sackmann, E. 2001 Oscillatory magnetic bead rheometer for complex fluid microrheometry. *Rev. Scient. Instrum.* **72**, 3626–3634.

Limozin, L. & Sackmann, E. 2002 Polymorphism of cross-linked actin networks in giant vesicles. *Phys. Rev. Lett.* **89**, 168103.

Lodish, H., Berk, A., Zipursky, S. L., Matsudaira, P., Baltimore, D. & Darnell, J. E. (eds) 1999 *Molecular Cell Biology*, 4th edn. New York: W. H. Freeman & Co.

MacKintosh, F. C., Käs, J. & Janmey, P. A. 1995 Elasticity of semiflexible biopolymer networks. *Phys. Rev. Lett.* **75**, 4425–4428.

Merkel, R., Simson, R., Simson, D. A., Hohenadl, M., Boulbitch, A., Wallraff, E. & Sackmann, E. 2000 A micromechanic study of cell polarity and plasma membrane cell body coupling in dictyostelium. *Biophys. J.* **79**, 707–719.

Morse, D. C. 1998*a* Viscoelasticity of concentrated isotropic solutions of semiflexible polymers. 1. Model and stress tensor. *Macromolecules* **31**, 7030–7043.

Morse, D. C. 1998*b* Viscoelasticity of concentrated isotropic solutions of semiflexible polymers. 2. Linear response. *Macromolecules* **31**, 7044–7067.

Morse, D. C. 1998*c* Viscoelasticity of tightly entangled solutions of semiflexible polymers. *Phys. Rev.* E **58**, R1237–R1240.

Morse, D. C. 2001 Tube diameter in tightly entangled solutions of semiflexible polymers. *Phys. Rev.* E **63**, 031502.

Pasternak, C., Spudich, J. A. & Elson, E. L. 1989 Capping of surface receptors and concomitant cortical tension are generated by conventional myosin. *Nature* **341**, 549–551.

Prost, J. 2002 The physics of *Listeria* propulsion. In *Physics of bio-molecules and cells* (ed. H. Flyubjerg, F. Jülicher, P. Ormos & F. David), pp. 215–236. Springer.

Sackmann, E., Bausch, A. R. & Vonna, L. 2002 Physics of composite cell membranes and actin based cytoskeleton. In *Physics of bio-molecules and cells* (ed. H. Flyubjerg, F. Jülicher, P. Ormos & F. David), pp. 237–284. Springer.

Schindl, M., Wallraff, E., Deubzer, B., Witke, W., Gerisch, G. & Sackmann, E. 1995 Cell-substrate interactions and locomotion of dictyostelium wild-type and mutants defective in three cytoskeletal proteins: a study using quantitative reflection interference contrast microscopy. *Biophys. J.* **68**, 1177–1190.

Schmidt, C. F., Bärmann, M., Isenberg, G. & Sackmann, E. 1989 Chain dynamics, mesh size, and diffusive transport in networks of polymerized actin: a quasielastic light scattering and micrfluorescence study. *Macromolecules* **22**, 3638–3649.

Smilenov, L. B., Mikhailov, A., Pelham, R. J., Marcantonio, E. E. & Gundersen, G. G. 1999 Focal adhesion motility revealed in stationary fibroblasts. *Science* **286**, 1172–1174.

Tempel, M., Isenberg, G. & Sackmann, E. 1996 Temperature induced sol-gel transition and microgel formation in α-actinin cross-linked networks: a rheological study. *Phys. Rev.* E **54**, 1802–1810.

Zheng, J., Lamoureux, P., Santiago, V., Dennerll, T., Buxbaum, R. E. & Heidemann, S. R. 1991 Tensile regulation of axonal elongation and initiation. *J. Neurosci.* **11**, 1117–1125.

Discussion

D. A. Weitz (*Department of Physics and DEAS, Harvard University, Cambridge, MA, USA*). The details of the frequency response measured by microrheology can depend sensitively on the size of the particle compared with the length-scales of the network. Do you think that the frequency response determined by magnetic bead microrheology correctly reflects the behaviour relevant for living cells?

E. Sackmann. At present, the smallest diameter of magnetic tweezers we have used is *ca.* 1 μm. The frequency response is thus expected to reflect correctly only the viscoelastic response experienced by intracellular compartments of similar size, such as vacuoles. Lysosomes which are much smaller (*ca.* 0.1 μm in diameter) can behave much differently. Systematic comparative studies of impedance spectra as a function of the ratio of the head to the mesh size and filament length by magnetic tweezers and (your) force-free microrheometry are required to answer this important and highly interesting question. The main advantage of the magnetic-tweezer techniques is that they enable measurements of the local yield stress within cells.

T. C. B. McLeish (*Department of Physics and Astronomy, University of Leeds, UK*). What is the criterion for bundling transition in networks in terms of persistence length and linker density? Does it correspond to more than one linker per L_{p}?

E. Sackmann. For dynamic cross-linkers such as α-actinin, the density of linkers required to induce bundling is larger than the density of naturally occurring cross-links. It would correspond to more than *ca.* 20 linkers per persistence length. This statement also holds for myosin in the presence of ATP. Bundling can occur at much lower densities for strong actin-linker binding, such as myosin in the presence of ADP. The density of linkers at which bundling occurs can also depend on the structure of the linker. Thus the fork-like linker filamin of muscles induces bundling already at densities equal to the density of the points of entanglement.

R. C. Ball (*Department of Physics, University of Warwick, Coventry, UK*). You noted that actin filaments have a persistence length of *ca.* 17 μm compared with cell dimensions of *ca.* 10 μm and of course the cortex is much thinner than that. This limits the relevance of comparison with networks where the mesh size exceeds the persistence length.

E. Sackmann. In our *in vitro* actin networks the mesh size is typically 0.4 μm, that is a factor of five larger than that in cells. The large mesh sizes are chosen to facilitate the micro-fluorescence experiments. The strategy is to establish scaling laws which are hoped to allow us to estimate the physical properties at physiological conditions. In fact, the viscoelastic moduli are also measured for small biologically relevant mesh sizes (cf. Hinner *et al.* 1998). Concerning the argument that the actin cortex is thinner than the persistence length, it should be noted that actin cortexes can be self-assembled in giant vesicles, which will enable future studies of viscoelastic

properties of such more biologically relevant actin networks (Limozin & Sackmann 2002).

P.-G. de Gennes (*Collège de France, Paris, France*). On the softening of actin by myosin, is this related to the observation by J. Käs that myosin plus actin plus ATP leads to a system with short relaxation times (moving one way in the tube rather than moving two ways)?

E. Sackmann. In our 'active' networks the myosin molecules are not aggregated, while as far as I understand they formed bundles in the experiments by Käs and co-workers. From our measurements, we can only conclude that the actin–myosin network is slightly softened in the low-frequency regime relative to the high-frequency regime. In fact, the plateau modulus is more pronounced in the presence of myosin, which is expected since myosin in the presence of ATP behaves as other dynamic cross-linkers (such as α-actinin).

M. Maaloum (*Institut Charles Sadron, Strasbourg, France*). When you analyse the dynamic of actin filament using ultramicroscopy, has the dynamic behaviour of the filament been modified by the colloids?

E. Sackmann. The diameter of the nano gold beads is 17 nm and is thus much smaller than the mesh sizes (greater than 100 nm). Therefore, the effect of the probes (1–3 per filament of 10 μm length) on the friction (for example, of a filament in its tube) is small. We also did not find any effect of the probe size on the time dependence of the MSD parallel and perpendicular to the tube axis (cf. figure 3).

A. J. Crompton (*Cybernetic Machine Group, British Computer Society, East Harptree, Bath, UK*). You refer to entanglement of actin molecules. Does this 'entanglement' refer to quantum coherence? Also, can you indicate the length of the 'entanglement' in amino acid units?

E. Sackmann. Entanglement means the formation of viscoelastic networks by steric interaction of flexible filaments that are long compared with the mesh size of the network. In amino acid units the entanglement length is of the order of the mesh size (cf. § 3). A double-stranded filament of 1 μm length is composed of *ca.* 40 actin monomers. Each monomer of molecular weight of 45 000 is composed of *ca.* 375 amino acids.